

Journal of Science and Technology

# Plasticisation Effect on Thermal, Dynamic Mechanical and Tensile Properties of Injection-Moulded Glass-Fibre/Polyamide 6,6

Nor Mas Mira Abd. Rahman, Aziz Hassan\*, Rosiyah Yahya

Department of Chemistry, Polymer and Composite Materials Research Laboratory, University of Malaya, 50603 Kuala Lumpur

\* *Corresponding e-mail: ahassan@um.edu.my*

---

## Abstract

Polymer composites of polyamide 6,6 reinforced with short glass fibre were prepared by injection moulding, conditioned under dry, 50% relative humidity and wet. Investigations by TGA, DSC, DMA and tensile tests were conducted. TGA results revealed that glass fibre loading in PA 6,6 improve the thermal stability of the composites. DSC analysis revealed that the incorporation of glass fibre and moisture into the PA 6,6 matrix resulted in a remarkable decrease in the degree of crystallinity. DMA results revealed the glass transition temperatures are sensitive to moisture absorption and their values move to a lower temperature upon exposure to moisture. Incorporation of glass fibre into the polyamide 6,6 gives rise to a significant improvement in tensile modulus and tensile strength, while tensile strain is reduced. Exposure to different environments from dry to wet conditions resulted in a decrease in the strength and modulus, while tensile strains decrease.

**Keywords:** Short-fibre composites, Plasticisation effects, Mechanical properties, Thermal properties, Dynamic mechanical analysis

---

## 1. INTRODUCTION

Thermoplastics such as poly(butylenes terephthalate), polypropylene and polyamides are excellent for use in composite materials for their performance-processability-profitability ratios. The mechanical properties of thermoplastic composites containing glass fibres have been the subject of much attention [1]. The properties of thermoplastic composites arise from the combination of fibre and matrix properties and the ability to transfer stresses across the fibre/matrix interphases [2].

In general, plastics and their corresponding composites are sensitive to changes in their environment and their mechanical properties may vary widely with conditions. In this respect, a very important role has been played by plasticisation, the process of depression of glass transition temperature and reduction of mechanical properties associated with the absorption of moisture or, more generally, of low molecular weight penetrant [1,3,4]. It is well known that environmental conditions have a profound effect on the viscoelastic properties of polymers. For hydrophilic materials, moisture is found to reduce stiffness and increase creep, presumably through plasticisation effect. The effects of constant moisture content on the mechanical properties of polymers have been widely studied and are fairly well understood [5]. In general, moisture diffusion in a composite depends on factors such as volume fraction of fibre, voids, viscosity of matrix, humidity and temperature [6].

Most polymers absorb moisture in humid atmosphere and when immersed in water. The absorption of moisture leads to the degradation of fibre matrix interfacial region and creating poor stress transfer efficiencies resulting in a reduction of mechanical and dimensional properties [7,8]. In fact, it is generally recognised that glass fibre-matrix interface is the determining factor of the reinforcement mechanism, particularly under wet conditions. The same observation was also reported by Thomason [9].

The objective of this work is to investigate the influence of glass as reinforcement in composites and the effect of conditioning (dry, 50% R.H. and wet) on thermal, dynamic mechanical and tensile properties of the injection moulded glass fibre reinforced polyamide 6,6 composites.

## **2. EXPERIMENTAL**

### **2.1. Materials, Specimen Preparation and Conditioning**

Materials used for the characterisation were Technyl® A216 (unreinforced polyamide 6,6) and Technyl® A216 V30 NAT (short glass fibre reinforced polyamide 6,6 composites, 16% fibre volume fraction,  $V_f$ ). Composites with three different fibre volume fractions,  $V_f$  of 4%, 8% and 12% were prepared by diluting of Technyl® A216 V30 NAT with Technyl® A216.

For the specimen preparation, a single gated double cavity, impact and tensile standard test bar mould was used in the moulding, using Boy® 50 tonne clamping force injection moulding machine. The dimensions of dumb-bell shaped tensile test pieces were in accordance with the ASTM Standard D638-80, type 1 [10].

For dry specimens, they were kept in vacuumed desiccators with silica gel immediately after the moulding. For 50% R.H. condition, the specimens were exposed to saturated sodium hydrogen sulphate ( $\text{NaHSO}_4$ ) solution environment in the desiccators for at least a month [11]. For wet conditioning, the samples were immersed in boiling water for at least 24 hours.

### **2.2. Determination of Thermal Properties (TGA and DSC)**

Thermogravimetric analysis (TGA) was investigated by using the TGA 6 Thermogravimetric Analyser (Perkin Elmer) to study the thermal decomposition behaviour of composites. Tests were done under nitrogen at a scan rate of  $10^\circ\text{C}/\text{min}$  in a programmed temperature range of  $50^\circ\text{C}$  to  $900^\circ\text{C}$ . A test sample of 5-10 mg was used for the run.

Differential scanning calorimetry (DSC) experiments were performed with a Diamond DSC (Perkin Elmer). Each sample was subjected to heating and cooling treatment at a scanning rate of  $10^\circ\text{C}/\text{min}$  under nitrogen atmosphere so as to prevent oxidation. A test sample of 5-10 mg was placed in an aluminium pan and tested over a temperature range of  $0^\circ\text{C}$  to  $290^\circ\text{C}$ .

### **2.3. Determination of Dynamic Mechanical Properties (DMA)**

The dynamic mechanical properties of specimens were analysed with a Dynamic Mechanical Analyser, DMA Q800 (Thermal Analysis Instrument). Test specimens were taken from the middle section of the injection moulded dumb-bell test bar and were subjected to three-point bending mode with a

support span of 50 mm. Measurements were conducted over a temperature range of  $-100^{\circ}\text{C}$  to  $150^{\circ}\text{C}$  with a heating rate of  $3^{\circ}\text{C}/\text{min}$  under a constant frequency of 1.0 Hz.

#### 2.4. Determination of Tensile Properties and Fracture Surface Morphology

Tensile tests were carried out using a Universal Testing Machine, Instron 4469 with a constant cross-head speed of 10 mm/min at room temperature of about  $25^{\circ}\text{C}$ . ASTM standard D638-80 [10] was used as a standard in calculating the tensile properties. After testing, the fractured surface was cut from the selected test specimen. A layer of gold was sputter-coated to improve the sample conductivity and avoid electrical charging during scanning electron microscopy (SEM) examination. JEOL Field Emission Auger Microprobe, JAMP-9500F was used to study the fractured surfaces under SEM mode.

### 3. RESULTS AND DISCUSSION

#### 3.1. Thermogravimetric Analysis (TGA)

Figures 1 and 2 show the TGA curves for all composites in the range of study under dry and wet conditions respectively. The thermal stability is characterised by the onset, derivative peak temperature and the temperatures at 50% of weight loss, which are referred as  $T_{\text{onset}}$ , DTP and  $T_{50\%}$ , respectively, as tabulated in Table 1.

**Table 1:** TGA thermogravimetric data of glass fibre composites under dry and wet conditions.

Sample	Decomposition Temperature ( $^{\circ}\text{C}$ )	$T_{50\%}$ ( $^{\circ}\text{C}$ )	$T_{\text{onset}}$ ( $^{\circ}\text{C}$ )	DTP ( $^{\circ}\text{C}$ )
$V_f$ 0% Dry	332 – 797	472	445	478
$V_f$ 0% Wet	301 – 799	426	416	426
$V_f$ 4% Dry	330 – 704	474	447	477
$V_f$ 4% Wet	303 – 705	477	447	478
$V_f$ 8% Dry	331 – 706	482	447	487
$V_f$ 8% Wet	302 – 685	480	445	479

The TGA curves show a single degradation step for all the composite samples. For the entire samples tested, thermal decomposition is completed at a temperature range of 685°C to 799°C. No further weight loss was observed after 799°C until the end of the temperature program at 850°C.

Gradual weight loss in the temperature range of 301°C to 799°C indicates the matrix content of the composites. The temperature range of 50°C to 200°C corresponds to the gradual weight loss due to evaporation of moisture. For wet samples, the percentage weight loss between 6% to 7% reflects the maximum moisture absorption by the samples. However, in dry samples, there is no existence of moisture in this temperature range, indicating no trap water/moisture by the polymer matrix. The decomposition of PA 6,6 matrix starts at a temperature of 332°C and reaches nearly 100% at 797°C.

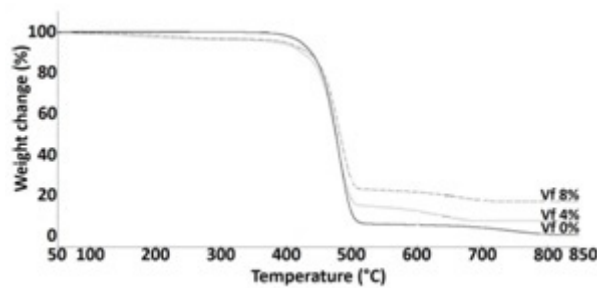


**Figure 1.** TGA thermographs of injection-moulded short glass fibre composites under dry condition.

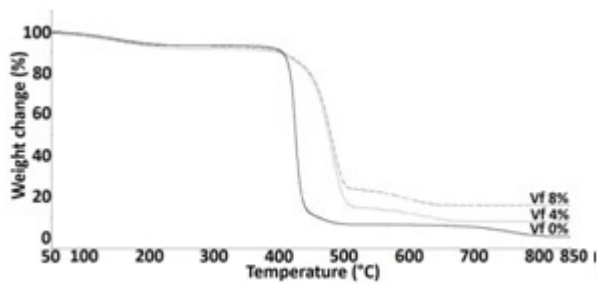


**Figure 2.** TGA thermographs of injection-moulded short glass fibre composites under wet condition.

It is a common practice to consider 50% weight loss as an indicator for structural destabilisation [12]. For composites under dry condition, the temperature at 50% weight loss,  $T_{50\%}$  for composites at both fibre loadings occur at about 2°C and 10°C higher than that of neat PA 6,6. For composites under

wet condition, the T50% were shifted by 51°C and 54°C for composites with fibre  $V_f$  of 4% and 8% respectively, compared to the pure matrix. Even though PA 6,6 matrix under wet condition shows a thermal stability remarkably lower than the matrix under dry condition, the TGA curves of PA 6,6 composites, for both 4% and 8%  $V_f$  glass fibre indicate a marked increase in thermal stability with respect to the wet matrix. These results suggest that the incorporation of glass fibre into the system has improved the structural destabilisation point of the composites.

According to the above results, the glass fibre loading in PA 6,6 produced positive effects on the thermal stability of the composites. The increment of  $DT_p$  values of the composites under both conditions compared to neat PA 6,6 (Table 1) also confirms the good thermal stability of these materials [13].

### 3.2. Differential Scanning Calorimetry (DSC)

The DSC thermograms of injection-moulded short glass fibre composites under dry and wet conditions are given in Figures 3 and 4 respectively. The DSC thermograms allow one to estimate the melting temperature ( $T_m$ ), crystallisation temperature ( $T_c$ ), enthalpy of melting ( $\Delta H_m$ ), enthalpy of crystalline ( $-\Delta H_c$ ) and also degree of crystallinity ( $X_c$ ) of the composites after the melt-crystallisation process by using a reference heat of fusion [14]. In this work, the reference value for the purely crystalline PA 6,6 is taken as 197 J/g ( $\Delta H_m^*$ ). These properties are tabulated in Table 2. DSC scans of all the samples were carried out for the first heating, cooling and second heating. However, only the results from the cooling and second heating are displayed and taken into consideration in the discussion. Ozdilek, et al. reported that the results from the second heating is useful to study as the first heating results may be influenced by the sample preparation and storage conditions [15].

The degree of crystallinity ( $X_c$ ) is calculated by using the following equation:

$$X_c = \frac{\Delta H_m}{\Delta H_m^*} \times 100 (\%) \quad (1)$$

where  $\Delta H_m$  and  $\Delta H_m^*$  are the enthalpies of composite specimen and purely crystalline PA 6,6 matrix respectively. Incorporation of glass fibres into the PA 6,6 matrix results in a remarkable decrease in  $X_c$  value than pure PA 6,6. As tabulated in Table 2,  $X_c$  of the composites under dry condition decreases from 37.5% for PA 6,6 matrix to 31.7% and 30.9% for 4% and 8%  $V_f$  glass

fibre composites respectively. This suggests that there is a significant change in the microstructure of the PA 6,6 matrix as a result of the incorporation of glass fibres [16]. The same behaviour is observed for composites under wet condition.

**Table 2:** DSC thermal properties of glass fibre composites under dry and wet conditions.

Sample	$T_m^a$ (°C)	$T_m^{\gamma}$ (°C)	$\Delta H_m$ (J/g)	$X_c$ (%)	$T_c$ (°C)	$-\Delta H_c$ (J/g)
$V_f$ 0% Dry	260	253	73.95	37.5	232	55.65
$V_f$ 0% Wet	260	253	64.55	32.8	232	46.37
$V_f$ 4% Dry	260	253	62.49	31.7	232	45.18
$V_f$ 4% Wet	260	254	57.85	29.4	232	38.84
$V_f$ 8% Dry	260	252	60.86	30.9	232	44.68
$V_f$ 8% Wet	260	254	56.40	28.6	232	40.01

In terms of conditioning, the incorporation of water into the system also reduces the degree of crystallinity. This is expected as the hydrogen bonds between the molecules are weakened. However, the existence of moisture is not the primary determining factor for polymer crystallinity as there is not much effect shown with the incorporation of glass fibre.

The melting temperature,  $T_m$  is mainly related to the degree of hydrogen bonding between the chains, which depends on the density of the amide groups. Thus, as the length of aliphatic groups between the amide link increases, the  $T_m$  will drop rapidly, for instance polyamide 6,6 melts at 260°C compared to polyamide 6,12 at 212°C [17].

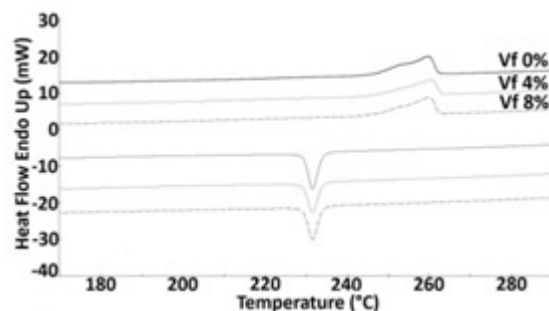


**Figure 3.** DSC thermograms of injection-moulded short glass fibre composites under dry condition (curves were shifted vertically for clarity).

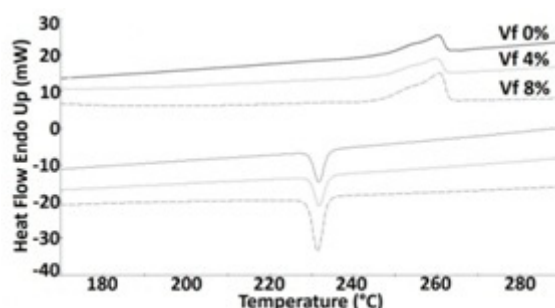


**Figure 4.** DSC thermograms of injection-moulded short glass fibre composites under wet condition (curves were shifted vertically for clarity).

Cooling of the composites by DSC resulted in one crystallisation peak. The heating scans show the presence of two melting peaks (Figures 3 and 4). The melting peak at/around 260°C could be attributed to the melting of the  $\alpha$ -crystalline portion of matrix ( $T_m^\alpha$ ). The one at/around 253°C, ( $T_m^\gamma$ ) probably indicates the melting of the thermodynamically unstable  $\gamma$ -crystalline [18-20]. Referring to Table 2, it can be seen that the presence of glass fibre did not produce any apparent effect on the melting temperature of the composites for both conditions. This suggests that the incorporation of glass fibre into the composites does not affect the degree of hydrogen bonding between the polymer chains.

The enthalpy of melting,  $\Delta H_m$  was determined at a heating rate of 10°C/min. The  $\Delta H_m$  is an important parameter since its magnitude is directly proportional to the overall level of  $X_c$  possessed by the polymer [21]. The  $\Delta H_m$  of unreinforced polyamide 6,6 at melting temperature is 73.95 J/g; decreases to 62.49 J/g and 60.86 J/g with the addition of 4% and 8%  $V_f$  glass fibre, respectively. This is expected due to reduction in degree of crystallinity of polymer matrix with the incorporation of fibres.

As for the crystalline peak temperature,  $T_c$  (Table 2), no significant changes in  $T_c$  values are observed with the incorporation of glass fibre and moisture into the system. However, the crystallinity enthalpy,  $-\Delta H_c$  of unreinforced polyamide 6,6 is 55.65 J/g, while with glass fibre of 4% and 8%  $V_f$  the  $-\Delta H_c$  decreases to 45.18 J/g and 44.68 J/g, respectively. Since the addition of glass fibre interfered with crystallisation, it is assumed that the decrease of  $-\Delta H_c$  is closely related to the decrease of  $X_c$  value [13]. Looking at the enthalpy of melting and enthalpy of crystallinity, the value of  $-\Delta H_c$  is less than the value of  $\Delta H_m$ . This is expected as some crystalline portions of polymer matrix do not



crystallise back. The presence of fibre may have restricted the crystallisation.

### 3.3. Dynamic Mechanical Properties

Results from dynamic mechanical analyses of the injection moulded composites are given in Figures 5 and 6, depicting  $\tan \delta$  against temperature curves. The thermomechanical data as extracted from these curves are tabulated in Table 3. From Figure 5, over a temperature range of  $-100^\circ\text{C}$  to  $150^\circ\text{C}$ , two transition regions as indicated by two damping maxima, are recorded for the dry specimens. These transitions are usually known as  $\beta$ -transition at a lower temperature and  $\alpha$ -transition at a higher temperature. The peak which is at maximum value of  $\tan \delta$  in  $\alpha$ -transition,  $T_\alpha$  is generally known as the glass transition temperature,  $T_g$ , while  $T_\beta$  is referred to temperature at the maximum value of  $\tan \delta$  in  $\beta$ -transition.  $W_{\sqrt{2}}$  is the width of the transition region ( $T_e - T_i$ ) at  $\tan \delta_{\max}/\sqrt{2}$  height.  $T_e$  and  $T_i$  are respectively the end and initial temperatures of the transition region. For wet specimens (Figure 6), only one transition,  $T_\alpha$  is recorded at much lower temperatures compared to the dry specimens.  $T_\beta$  is eliminated or reduced to below  $-100^\circ\text{C}$  and not detected under the present test temperature range.

**Table 3:** DMA thermomechanical data of glass fibre composites under dry and wet conditions.

Sample	Vf (%)	A-transition					$\beta$ -transition $T_\beta$ ( $^\circ\text{C}$ )
		$\tan \delta_{\max}$ ( $\times 10^{-2}$ )	$T_\alpha$ ( $^\circ\text{C}$ )	$T_i$ ( $^\circ\text{C}$ )	$T_e$ ( $^\circ\text{C}$ )	$W_{\sqrt{2}}$ ( $^\circ\text{C}$ )	
$V_f$ 0% Dry	0	8.68	50	28	77	49	-69
$V_f$ 4% Dry	4	6.80	40	20	80	60	-70
$V_f$ 8% Dry	8	4.88	50	20	83	63	-70
$V_f$ 12% Dry	12	4.97	52	16	128	112	-69
$V_f$ 0% Wet	0	11.42	-13	-28	8	36	-
$V_f$ 4% Wet	4	9.10	-16	-30	7	37	-
$V_f$ 8% Wet	8	7.40	-16	-32	8	40	-
$V_f$ 12% Wet	12	6.37	-16	-32	7	39	-

#### 3.3.1 Effect of $V_f$ on $T_g$ and $\tan \delta$ (Dry and Wet Specimens)

As shown in Figure 5, the incorporation of fibres produces no significant trend in displacement of the  $\alpha$ -relaxation peak for the dry specimens. Composite with 4%  $V_f$  of glass fibre shows the lowest  $T_g$  ( $40^\circ\text{C}$ ), compared to the other

compositions (50°C and 52°C for  $V_f$  of 8% and 12% respectively). It is suggested that the incorporation of lower fraction of glass fibre may only give notching effect to the composite. They may introduce a microvoid in the composites and instead of reinforcing the matrix, it weakens the composites. There is no change in  $T_g$  of composite at  $V_f$  of 8% and only a negligible increase of 2°C at  $V_f$  of 12%. On the other hand, the presence of the glass fibre reduces the magnitude of  $\tan \delta_{\max}$  values dramatically. Higher reduction for composites with higher fibre loadings is believed due to the strengthening effect by the fibres.  $\tan \delta_{\max}$  of reinforced composites shows a maximum decrease of about 44% compared to the pure matrix (0.0868 to 0.0488). In this instance, the incorporation of fibres acts as barriers to the mobility of polymer chain, leading to lower degree of molecular motion and hence lower damping characteristics [22]. Another possible reason is that there is less matrix by volume to dissipate the vibration energy.

For the effect of  $V_f$  on wet specimens, the same trend as for the dry specimens is observed in terms of stability in  $T_g$  values and reduction in  $\tan \delta_{\max}$ .  $T_g$  of all composite specimens recorded a 3°C decrease compared to the pure matrix (-13°C to -16°C). This is believed due to the existence of moisture that weakens the polymer matrix. By chance,  $\tan \delta_{\max}$  of reinforced composites show a maximum decrease of also 44% compared to the pure matrix (0.1142 to 0.0637); same magnitude of change as that observed for the dry specimens.

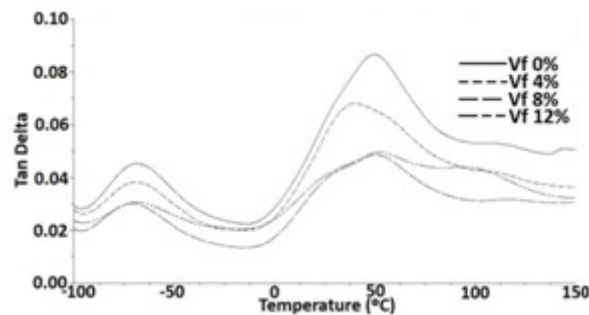


**Figure 5.** DMA tan delta–temperature behaviour of injection-moulded short glass fibre composites under dry condition

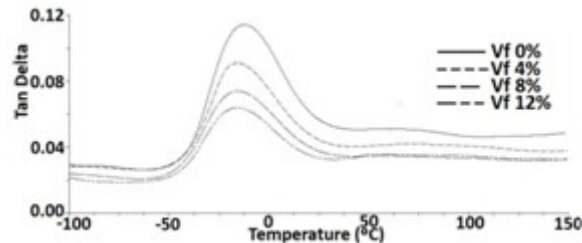


**Figure 6.** DMA tan delta–temperature behaviour of injection-moulded short glass fibre composites under wet condition.

### 3.3.2 Effect of Moisture on $T_g$ and $\tan \delta$ (Wet and Dry Specimen)

Water uptake decreases the  $T_g$  of pure matrix drastically compared to the dry specimens, from 50°C to –13°C (reduction of 63°C). For composite specimens,  $T_g$  values reduce from between 40°C and 52°C to –16°C, with a magnitude of between 56°C to 68°C. Water uptake also increases the values of  $\tan \delta_{\max}$ . For pure matrix, the increase in  $\tan \delta_{\max}$  is 32%, from 0.0868 to 0.1142. For composite specimens, the increases are between 28% to 51%. From these figures, it can be concluded that the major contributing factor that leads to the reduction in  $T_g$  and increase in  $\tan \delta_{\max}$  is the moisture uptake, not the fibre loadings.

### 3.3.3 Effect of $V_f$ on $\alpha$ -Transition Region.

As can be seen in Figures 5 and 6; and Table 3,  $\tan \delta_{\max}$  decrease with the increase in fibre loadings for both dry and wet specimens. This decreases the  $\tan \delta_{\max}/\sqrt{2}$  height, decreases the  $T_i$  and increases the  $T_c$  and eventually increases the width of  $\alpha$ -transition region ( $W_{\sqrt{2}}$ ). For the dry specimens, dramatic increase in  $W_{\sqrt{2}}$  is shown by samples at all fibre loadings, whereby  $V_f$  of 4%, 8% and 12% recorded an increase of  $W_{\sqrt{2}}$  by 22%, 29% and 129% compared to the pure matrix (from 49°C to 60°C, 63°C and 112°C respectively). However, for the wet specimens, there are negligible differences in their  $T_i$ ,  $T_c$  and  $W_{\sqrt{2}}$ . Composites with  $V_f$  of 4%, 8% and 12% recorded an increase of  $W_{\sqrt{2}}$  by only 3%, 11% and 8% respectively compared to the pure matrix (from 36°C to 37°C, 40°C and 39°C respectively). These trends indicate that, under dry condition, glass fibre is a major controlling factor in damping properties. In contrary, under wet condition, fibre becomes less important and matrix is the controlling factor.

Comparing Figures 5 and 6, and data in Table 3, it can be seen that the

$\tan \delta$  peaks of  $\alpha$ -transition for both unreinforced and reinforced PA 6,6 shift to lower values when exposed to humid environment. Since humidity acts as a plasticiser, this induces a further increase in the amorphous chain mobility in the material and hence reduces Tg significantly [23].

### 3.4 Tensile Properties

Tensile properties of all composites specimen and their Property Index (PI) values are tabulated in Table 4. The PI values, where the property for the dry specimen was taken as reference, were calculated using the following general

$$\text{Property Index} = \frac{\left(\frac{P_c}{V_f}\right)}{\left(\frac{P_c^r}{V_f^r}\right)} \quad (2)$$

where,  $P_c^r$  and  $V_f^r$  are the respective property and fibre volume fraction of a reference composite, and  $P_c$  and  $V_f$  are the corresponding property and fibre volume fraction of the composite from which a comparison is to be made.

**Table 4.** Tensile properties glass fibre composites.

Sample	Tensile strength		Tensile modulus		Tensile strain	
	Value (MPa)	PI	Value (GPa)	PI	Value (%)	PI
$V_f$ 0% Dry	31.45	1.00	1.54	1.00	91.50	1.00
$V_f$ 0% 50%RH	40.04	1.27	1.13	0.73	117.88	1.29
$V_f$ 0% Wet	36.03	1.15	0.39	0.25	231.60	2.53
$V_f$ 4% Dry	59.66	1.00	1.85	1.00	5.94	1.00
$V_f$ 4% 50%RH	49.06	0.82	1.47	0.79	4.55	0.77
$V_f$ 4% Wet	40.18	0.82	0.69	0.47	32.89	7.23
$V_f$ 8% Dry	95.07	1.00	2.64	1.00	8.42	1.00
$V_f$ 8% 50%RH	83.87	0.88	2.33	0.88	5.79	0.69
$V_f$ 8% Wet	54.31	0.57	1.08	0.41	15.90	1.89
$V_f$ 12% Dry	151.23	1.00	3.74	1.00	7.18	1.00
$V_f$ 12% 50%RH	117.12	0.77	3.07	0.82	8.92	1.24
$V_f$ 12% Wet	75.73	0.50	1.84	0.49	11.09	1.54

In the tensile tests, all specimens broke in a brittle manner, except for some which indicate ductility as that shown by the unreinforced polyamide 6,6 specimens (under all conditions). In the order of increasing fibre loading (Table 4), the tensile strength and tensile modulus increase. These results confirm that the fibres act as an effective reinforcing agent for PA 6,6, giving rise to a more rigid material [22]. Haneefa, *et al.* [24] suggested that the addition of glass fibre increases the effective mechanical interlocking, which in turn increases the frictional force between the fibre and matrix. Increasing the amount of glass fibre leads to higher stiffness of composite thus more energy is required to break the specimens. The applied load is transferred to the strong and stiff fibres through the fibre-matrix interface. As the volume fraction of fibre reinforcement in composites increases, more fibre-matrix interfacial area is created and the more applied load is transferred to the fibre by the interface [16]. Thus, it is more difficult to break the specimen and hence results in greater tensile strength and tensile modulus. The composites at all fibre loadings at the same condition show similar trend.

However, if the fibre-matrix adhesion is weak, cracks tend to form at the interface and link up quickly through highly stressed sections of the matrix, resulting in premature failure of the composite. Nevertheless, it can be seen that the composite strength and composite modulus increase with an increase in the fibre loading. This shows that fibre-matrix adhesion for these composites is strong. Microscopic studies prove, it can be seen clearly that there is a good fibre-matrix bonding at glass fibre surfaces (Figure 7). Other researchers [2,25] have also reported equivalent trend of results and showed that the fibre-matrix interfacial adhesion strength increases with the PA 6,6 concentrations in the matrix system. Generally, tensile strength and tensile modulus increase with an increase in fibre loading.

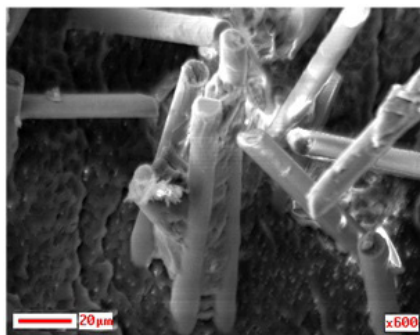


**Figure 7.** SEM micrograph of tensile fracture surface of glass fibre composite under dry as moulded condition.

All specimens of fibre-filled materials failed at strain below the normal yield strain of the matrix. The fracture strain decreases with increase in fibre volume fraction. This trend is also reported by Thomason, *et al.* [26] and explained that the stress concentrations at the fibre ends lead to matrix cracking, which ultimately leads to failure when the surrounding matrix and fibres can no longer support the increased load caused by the local failure.

Previous studies [27,28] have also reported the decrement in fracture strain as the  $V_f$  increases. Due to the introduction of fibres, the composites become less ductile as the molecular rearrangement does not have time to take place. The notching effect of the fibres is also important in which considerable stress concentration is induced in the matrix at the fibre end and matrix flow is constrained by adjacent fibres. Takahashi and Choi [29] who studied on the failure mechanisms proven that under loading of tensile stress, the cracks start at the fibre ends and propagate along the fibre-matrix interface or cross through the matrix and finally the failure takes place.

At the same fibre loading, samples in wet condition show lowest tensile strength and tensile modulus compared to other conditions. This is expected, as water causes the fibre to swell altering its dimensions and in turn changes the size, shape, stiffness and permeability. Moisture acts as a plasticiser that reduces the entanglement and bonding between molecular chains, therefore increases their volume and mobility [30]. As a result, the absorbed water lowers the tensile modulus, but increases the elongation at break. Compared to the dry specimen, the fracture strain of 50% RH specimens increased reasonably; however, drastically increased for wet specimens, for all unfilled and filled materials (refer to Table 4).

Mohd Ishak, *et al.* [16] reported that the absorbed moisture significantly changed the fracture mode from being brittle to a ductile fracture, resulting in reduction of the tensile strength and tensile modulus. In other studies, Thomason [31] also reported that the reduction in tensile strength and tensile modulus is due to the existence of water which lowers the stress transfer capability of the fibre-matrix interface.

The failure strain value for the wet specimens was found to increase compared to the dry specimens. An increase in fracture strain is evident when moisture increases from dry to wet condition. The increase in failure strain upon exposure of the samples to a wet environment can be attributed to the plasticisation of nylon 6,6 caused by moisture absorption. In the presence of

moisture, lubrication effect takes place allowing the polymer chains to slip past each other. The hydrogen bonding between moisture and matrix formed in the composites and the dipole–dipole interaction between matrix and fibres become less effective [32]. When a fibre breaks, the load it supports is transferred to the surrounding fibres by matrix resin. As the relative moisture absorbed increases, adhesion between matrix resin and fibre becomes poorer; hence the matrix can no longer effectively distribute the applied load over an appreciable length of the adjacent fibres. Therefore, less occurrence of fibre breakage and consequently, fracture strain of composites increase.

From SEM image in Figure 8(A), no matrix deformation is observed and there is also some indication of matrix cracking. This explains the extreme brittle behaviour of the composite during tensile test for dry as-moulded specimens. For wet specimens, picture shown in Figure 8(B) indicate that the surface of some fibres is smooth and there is the matrix yielding which illustrates the physical damage of the interphase and debonding between fibre and matrix. Reports revealed that water molecules act as a plasticiser agent in the composite material, which normally leads to an increase of the maximum strain for the composites after water absorption [33].

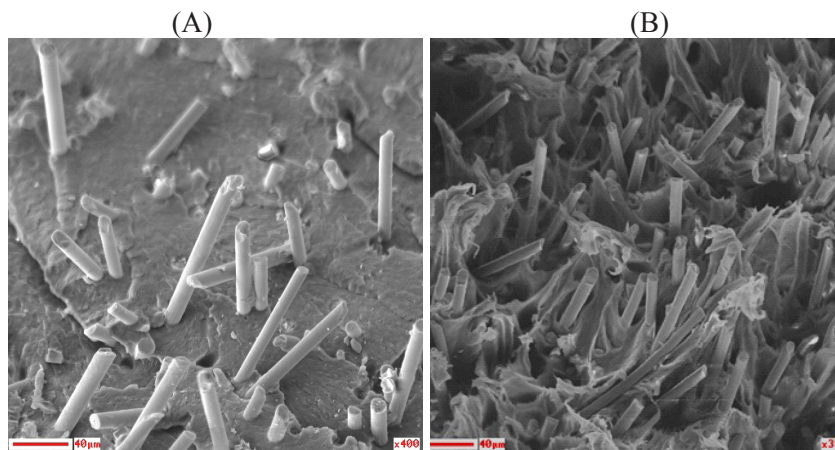


**Figure 8.** SEM micrographs of tensile fracture surface of glass fibre composites under (A) dry as-moulded and (B) wet conditions.

#### 4 CONCLUSIONS

The degree of crystallinity of polymer is reduced with incorporation of glass fibre in the composites. The  $T_g$  value is not significantly altered by incorporation of glass fibre into the system. However, its value is reduced with moisture content. Tensile strength and tensile modulus are increased with increase in  $V_f$ . However, fracture strain of composites under all conditions is decreased in the order of increasing fibre loading. At the same fibre loading, specimen in wet condition showed the lowest tensile strength and tensile modulus. With the absorption of water, tensile strength and tensile modulus decreased; fracture strain increased.

#### Acknowledgements

We thank the Government of Malaysia and the University of Malaya as the work reported in this paper was supported by grants IRPA 33-02-03-3054 and FP017/2008C.

#### REFERENCES

- [1] Cotugno, S., Mensitieri, G., Musto, P., Nicolais, L. (2002). "Water Sorption & Transport in Polymers" in Proceedings of the Conference on Nylon and Ropes for Mountaineering and Caving. Torino.
- [2] Thomason, J.L. (2001). "Micromechanical Parameters from Macromechanical Measurements on Glass Reinforced Polyamide 6,6" in Compos Sci Technol, Vol. 61. pp. 2007-2016.
- [3] Sakellariou, P., Hassan, H., Rowe, R.C. (1994). "Plasticization and Interactions of Polyethylene Glycol 6000 with Hydroxypropyl Methyl Cellulose/Polyvinyl Alcohol Blends" in Int J Pharm, Vol. 102. No. 1-3 pp. 207-211.
- [4] Sakellariou, P., Hassan, A., Rowe, R.C. (1994). "Interactions and Partitioning of Diluents/Plasticisers in Hydroxypropyl Methylcellulose and Poly(vinyl alcohol) Homopolymers and Blends" in Part II: Glycerol, Colloid Polym Sci, Vol. 272. No. 1 pp. 48-56.



- [5] Crosby, J.M, Drye, T.R. (1987). “Fracture Studies of Discontinuous Fibre Reinforced Thermoplastic Composites” in *J Reinf Plast Compos*, Vol. 6. No. 2 pp. 162-177.
- [6] De La Osa, O. (2006). “Effect of Hygrothermal History on Water and Mechanical Properties of Glass/vinylester Composites” in *J Compos Mater*, Vol. 40. pp. 2009-2023.
- [7] Dhakal, H.N., Zhang, Z.Y., Richardson, M.O.W. ((2007). “Effect of Water Absorption on the Mechanical Properties of Hemp Fibre Reinforced Unsaturated Polyester Composites” in *Compos Sci Technol*, Vol. 67. pp. 1674-1683.
- [8] Yang, G.C., Zheng, H.M., Li, J.J., Jian, N.B., Zhang, W.B. (1996). “Relation of Modification and Tensile Properties of Sisal Fibre” in *Acta Sci Nat Uni Sunyatseni*, Vol. 35. pp. 53-57.
- [9] Thomason, J.L. (1995). “The Interface Region in Glass Fibre-Reinforced Epoxy Resin Composites: 2. Water Absorption, Voids and the Interface” in *Composites*, Vol. 26. pp. 477-485.
- [10] ASTM D638-80. Standard Test Method for Tensile Properties of Plastics, Part 35. pp. 228-244.
- [11] ASTM D618-00. Standard Practice for Conditioning Plastics for Testing, pp. 39-42.
- [12] Chisholm, N., Mahfuz, H., Rangari, V.K., Ashfaq, A., Jeelani, S. (2005) “Fabrication and Mechanical Characterization of Carbon/SiC-Epoxy Nanocomposites” in *Compos Struct*, Vol. 67. No. 1 pp. 115-124.
- [13] Lee, S.Y., Kang, I.A., Doh, G.H., Kim, W.J., Kim, J.S., Yoon, H.G., Wu, Q. (2008). “Thermal, Mechanical and Morphological Properties of Polypropylene/Clay/Wood Flour Nanocomposites” in *Express Polym Lett*, Vol. 2. No. 2 pp. 78-87.
- [14] Elzein, T., Brogly, M., Schultz, J. (2002). “Crystallinity Measurements of Polyamides Adsorbed as Thin Films” in *Polymer*, Vol. 43. pp. 4811-4822.

- [15] Ozdilek, C., Kazimierczak, K., Van der Beek, D., Picken, S.J. (2004). "Preparation and Properties of Polyamide-6-Boehmite Nanocomposites" in *Polymer*, Vol. 45. pp. 5207-5214.
- [16] Mohd Ishak, Z.A., Ariffin, A., Senawi, R. (2001). "Effects of Hygrothermal Aging and a Silane Coupling Agent on the Tensile Properties of Injection Moulded Short Glass Fibre Reinforced Poly(butylenes terephthalate) Composites" in *Eur Polym J*, Vol. 37. pp. 1635-1647.
- [17] Garbassi, F., Po, R. (2003). "Engineering Thermoplastics-Overview" In Mark, H.F., editor. *Encyclopedia of Polymer Science and Technology*, Vol. 2. No. 3. *John Wiley and Sons*, New York.
- [18] Klata, E., Van de Velde, K., Krucinska, I. (2003). "DSC Investigations of Polyamide 6 Hybrid GF/PA 6 Yarns and Composites" in *Polym Test*, Vol. 22. pp. 929-937.
- [19] Penel-Pierron, L., Depecker, C., Se'gue'la, R., Lefebvre, J.M. (2001). "Structural and Mechanical Behaviour of Nylon 6 Films Part I. Identification and Stability of the Crystalline Phases" in *J Polym Sci B-Polym Phys*, Vol. 39. pp. 448-449.
- [20] Edith Turi, A. (1997). *Thermal Characterization of Polymeric Materials*. *Polytechnic University Brooklyn*, New York.
- [21] Sichina, W.J. (1994). "Prediction of End-Use Characteristics of Polyethylene Materials Using Differential Scanning Calorimetry" in USA: Application Briff DSC-11.
- [22] Manchado, M.A.L., Biagiotti, J., Kenny, J.M. (2002). "Comparative Study of the Effects of Different Fibres on the Processing and Properties of Polypropylene Matrix Composites" in *J Thermoplast Compos Mater*, Vol. 15. pp. 337-353.
- [23] Aitken, D., Burkinshaw, S.M., Cox, R., Catherall, J., Litchfield, R.E., Price, D.M., Todd, N.G. (1991). "Determination of the Glass Transiti on Temperature of Wet Acrylic Fibres using Dynamic Mechanical Analysis" in *J Appl Polym Sci: Appl Polym Symp*, Vol. 47. pp. 263-269.

- [24] Haneefa, A., Bindu, P., Aravind, I., Thomas, S. (2008). “Studies on Tensile and Flexural Properties of Short Banana/Glass Hybrid Fibre Reinforced Polystyrene Composites” in *J Compos Mater*, Vol. 42. pp. 1471-1489.
- [25] Fu, S.Y., Lauke, B., Zhang, Y.H., Mai, Y.W. (2005). “On the Post-Mortem Fracture Surface Morphology of Short Fibre Reinforced Thermoplastics” in *Compos Part A – Appl Sci Manuf*, Vol. 36. pp. 987-994.
- [26] Thomason, J.L., Vlug, M.A., Schipper, G., Krikort, H.G.L.T. (1996). “Influence of Fibre Length and Concentration on the Properties of Glass Fibre-Reinforced Polypropylene: Part 3. Strength and Strain at Failure” in *Compos Part A – Appl Sci Manuf*, Vol. 27. pp. 1075-1084.
- [27] Curtis, P.T., Bader, M.G., Bailey, J.E. (1978). “The Stiffness and Strength of a Polyamide Thermoplastic Reinforced with Glass and Carbon Fibres” in *J Mater Sci*, Vol. 13. pp. 377–390.
- [28] Mouhmid, B., Imad, A., Benseddiq, N., Benmedakhene, S., Maazouz, A. (2006). “A Study of Mechanical Behaviour of a Glass Fibre Reinforced Polyamide 6,6: Experimental Investigation” in *Polym Test*, Vol. 25. pp. 544-552.
- [29] Takahashi, K., Choi, N.S. (1991). “Influence of Fibre Weight Fraction on the Failure Mechanisms of Poly(ethylene terephthalate) Reinforced by Short Glass Fibres” in *J Mater Sci*, Vol. 26. pp.4648–4656.
- [30] Kohan, M. (1995). *Nylon Plastics Handbook*. Hanser Gardner Publications Inc., New York.
- [31] Thomason, J.L. (2009). “The Influence of Fibre Length, Diameter and Concentration on the Impact Performance of Long Glass-Fibre Reinforced Polyamide 6,6” in *Compos Part A – Appl Sci Manuf*, Vol. 40. pp. 114-124.
- [32] Sombatsompop, N., Chaochanchaikul, K. (2004). “Effect of Moisture Content on Mechanical Properties, Thermal and Structural Stability and Extrudate Texture of Poly(vinyl chloride)/Wood Sawdust Composites” in *Polym Int*, Vol. 53. pp. 1210–1218.

- [33] Stamboulis, A., Baillie, C.A., Peijs, T. (2001). “Effects of Environmental Conditions on Mechanical and Physical Properties of Flax Fibres” in *Compos Part A – Appl Sci Manuf*, Vol. 32. pp. 1105–1115.